Appl. Phys. B 76, 467–471 (2003)
DOI: 10.1007/s00340-003-1118-6

Applied Physics B
Lasers and Optics

T. WITTE
K.L. KOMPA
M. MOTZKUS✉

Femtosecond pulse shaping in the mid infrared by difference-frequency mixing

Max-Planck-Institut für Quantenoptik, Hans-Kopfermann-Str. 1, 85748 Garching, Germany

Received: 12 December 2003
Published online: 3 April 2003 • © Springer-Verlag 2003

ABSTRACT The generation of programmable complex femtosecond pulses in the mid infrared (3–10 μm) with high precision is reported. Designed pulse shapes in the near infrared (1–1.6 μm) are transferred to the mid infrared via difference-frequency mixing with a second infrared pulse spectrally narrowed in a zero-dispersion compressor. In particular, pulse sequences with variable relative phases have been obtained. The control of the pulse properties is achieved purely electronically, allowing for implementation into a feedback loop.

PACS 42.65.Re; 42.65.Ky; 42.72.Ai

1 Introduction

There has recently been much interest in the generation of shaped femtosecond (fs) laser pulses in the mid infrared (MIR) [1–4]. This is motivated by the expectation that such pulses will allow for coherent control, for instance, of molecular vibrational excitations in the ground electronic state [5] or elementary excitations in condensed matter systems [6, 7]. In particular, the feasibility of electronically programmable fs MIR pulses suggests an implementation into concepts of feedback-control technology [8]. Recent progress in the control of vibrational excitation [9] as well as molecular dissociation [10] effected by resonant MIR fs laser pulses further underlines the potential of coherent control studies for chemical dynamics.

Other than in the visible and near-infrared wavelength regimes, where direct pulse-shaping techniques employing liquid-crystal masks (LCMs) or acousto-optical modulators (AOMs) are now routinely used, possible approaches to generate complex pulse shapes in the mid IR, as well as in the UV [11], are more intricate. The paramount obstacle is that these shaping devices are not transparent (LCM) or show very low diffraction efficiency (AOM) in these wavelength regimes, which obstructs the direct modulation of the electric field transients. Whereas, for the UV, deformable mirrors [12] might prove a potentially promising technology to achieve phase modulations, this approach cannot yet be employed in the MIR, since here the deformations necessary to effect significant phase modulations are much larger. For the MIR regime, several alternative schemes are viable. For pure amplitude shaping, the direct blocking of spectral components in a 4-f setup [13] is a simple approach. Similarly, for quadratic phase modulations (linear chirp) a 4-f setup can be used if the distance between the dispersing grating and the focussing mirror is adjustable. This has been demonstrated with the MIR output from a free-electron laser [14]. However, the above are concepts for stationary modulations, which also require mechanical adjustments when applied and do not offer access to more complex transients in the MIR.

A first example of a programmable MIR pulse was achieved by an intricate difference-frequency mixing (DFM) scheme in GaSe, which involved the mixing and shaping of the spectral tail and edge of a single 13-fs, 800-nm pulse to result in a double pulse at 13 μm [15]. Such a pulse was used to investigate intersubband excitations in semiconductor quantum wells [7]. However, with this shaping concept, only picojoule pulses were produced, and the limited bandwidth of the 800-nm pulse hampers the generation of pulses in the spectroscopically interesting region of 3–10 μm.

An alternative approach is represented by indirect shaping techniques, by which we mean the transfer of an intentionally shaped fs pulse from one wavelength region to another by a parametric process, which involves a second laser pulse without any complex phase or amplitude structure [1, 3, 16, 17]. In the first step, any desired pulse shape is obtained by direct pulse shaping in a spectral region which allows the use of a liquid-crystal mask. The second step is marked by the parametric, or frequency, mixing process, through which a modulated pulse in a completely different frequency range is obtained. Such an approach allows for electronically controlled generation of complex electric fields not accessible with the stationary schemes mentioned above. We have recently demonstrated this capacity in two cases: first, a white-light continuum was shaped and used in an optical parametric process to generate phase-locked two-color double pulses in the visible [16]. Second, the signal output of an IR op-

✉ Fax: +49-89/32905-200, E-mail: mcm@mpq.mpg.de

tical parametric amplifier was directly shaped and mixed with a broadband chirped idler pulse to produce controlled and programmable pulse shapes in the 3–10-μm wavelength regime [1]. Programmable amplitude and phase modulations as well as pulse sequences were achieved with pulse energies of up to 1 μJ.

The key aspect in transferring a specific pulse shape via a mixing process is the fact that the resulting electric field transient will be the result of a convolution of the two input fields with given amplitude and phase properties. The central question is then to which extent the original pulse shape is conserved during the transfer process. In the present communication, we will discuss a significantly improved transfer scheme and present MIR pulse shapes of previously unattained complexity, with an emphasis on pulse sequences with variable relative phases.

2 Experiment

MIR fs light pulses are generated by mixing signal and idler pulses from a traveling wave optical parametric amplifier (pumped with 800-nm, 100-fs pulses from a standard amplified Ti:Sa laser system) in a 1-mm $AgGaS_2$ crystal (type II). The signal and idler wavelength ranges are 1.1–1.6 μm and 1.6–2.9 μm, respectively, resulting in MIR pulses in the 3–10-μm regime. Mathematically, the process of depleted DFM is usually described by

$$\partial_z \tilde{E}_\mathrm{D}(\omega_\mathrm{D}) \propto \int_{\omega_\mathrm{S}^0-\Delta\omega}^{\omega_\mathrm{S}^0+\Delta\omega} \chi^{(2)} \cdot \tilde{E}_\mathrm{S}^*(\omega_\mathrm{S}) \tilde{E}_\mathrm{I}(\omega_\mathrm{S}-\omega_\mathrm{D}) \mathrm{e}^{\mathrm{i}\Delta k z}\, \mathrm{d}\omega_\mathrm{S}\,, \tag{1}$$

where the indices S, I and D indicate signal, idler and DFM pulses, respectively, and $\chi^{(2)}$ denotes the frequency-dependent nonlinear coefficient of the crystal. Energy conservation requires $\omega_\mathrm{D} = \omega_\mathrm{S} - \omega_\mathrm{I}$, and the phase-matching requirement yields $\Delta k = k_\mathrm{D} - k_\mathrm{S} + k_\mathrm{I}$. We have defined ω_S^0 as the center frequency of the signal pulse and $2\Delta\omega$ as a frequency range which comprises all signal frequencies with nonzero amplitude. The two input fields are described by two equations similar to (1). Each frequency component ω_D represents a weighted sum of contributions from pairs of frequencies (ω_S, ω_I), which satisfy energy conservation. Weighting factors for the output electric field are: (i) the intensity of each input frequency and (ii) the properties of the nonlinear crystal that determine the strength of the interaction. Since the electric fields in (1) are complex, their phases give rise to interferences in the sum represented by the integral, and therefore likewise influence the output electric field. With (1), the task of indirect pulse shaping can now be clarified: if one provides a phase- and amplitude-modulated signal field, a designed modulated MIR pulse will result from the (possibly nontrivial) convolution with the idler field. As a prerequisite, the idler and the shaped signal field must temporally fully overlap. The idler pulse therefore must be stretched in time. In our first approach, the idler, having the bandwidth of a 100-fs pulse, was chirped to match the time duration of a shaped signal pulse [1]. The idler electric field in (1) is then highly complex. The impact on the resulting MIR field may in this case be discussed on the basis of three examples: first, if both the idler and signal pulses are negatively chirped, then the difference frequency over the pulse's time duration may even be constant, resulting in a narrow-band unchirped MIR pulse [18]. Second, a one-color double pulse mixed with a chirped idler pulse will result in a two-color MIR double pulse, since the individual pulses from the signal sequence will 'see' different central frequencies of the idler pulse [1]. Third, amplitude modulations cannot be directly transferred with a broadband idler, since there are many contributions to one MIR frequency in the integral of (1).

From these examples we conclude that, for optimized indirect MIR pulse shaping, the convolution, and thus the generation of specific electric transients in the MIR, must be simplified. In the ideal case, the idler is a monochromatic wave. Then (1) is simplified to

$$\partial_z \tilde{E}_\mathrm{D}(\omega_\mathrm{S}-\omega_\mathrm{I}) \propto \chi^{(2)} \cdot \tilde{E}_\mathrm{S}^*(\omega_\mathrm{S}) E_\mathrm{I}(\omega_\mathrm{I}) \mathrm{e}^{\mathrm{i}\Delta k z}. \tag{2}$$

Hence, the individual features of the signal pulse would be quantitatively and qualitatively transferred to the MIR. An approximation to such conditions is represented by employing narrow-band idler pulses, which are simultaneously Fourier-limited, i.e. possess a constant spectral phase.

Our realization of such a scheme is schematically depicted in Fig. 1. The signal is routed through a LC mask (CRI SLM-256 MIR) in an all-reflective 4-f setup [19]. The mask, which is a stack of two separate $N = 128$-pixel arrays, can independently influence spectral attenuation and phase within the limitations of a discrete shaping device, as has been described elsewhere [20, 21]. The idler is also routed through a 4-f setup

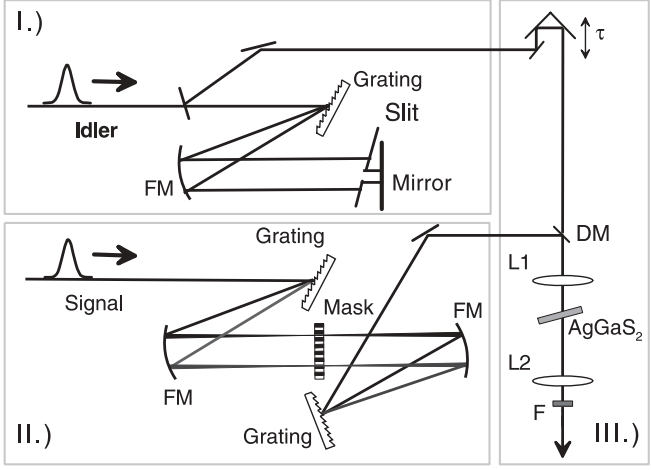

FIGURE 1 Diagram of experimental setup. I. Idler-shaping setup: FM, focussing mirror with $f = 300$ mm; grating with $1/d = 200$ lines/mm. II. Signal-shaping setup: FM, focussing mirror with $f = 300$ mm; grating with $1/d = 400$ lines/mm; mask CRI SLM-256. III. Difference-frequency generation in $AgGaS_2$ (type II, cut at 50°): DM, dichroic mirror; L1, CaF_2 lens, $f = 250$ mm; L2: BaF_2 lens, $f = 250$ mm; F, filter

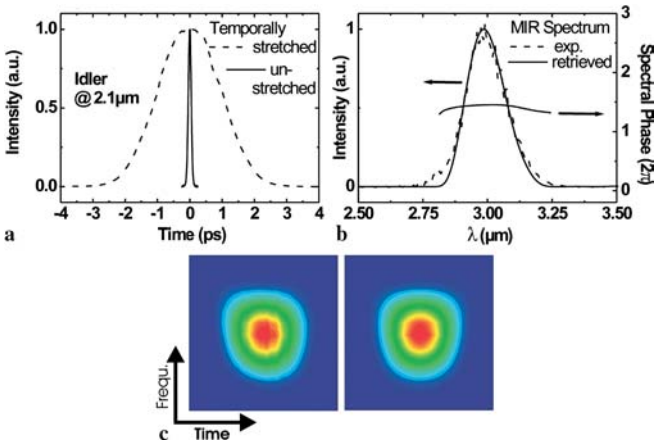

FIGURE 2 **a** Idler autocorrelation trace before and after spectral narrowing at 2.1 µm. **b** Spectrum and spectral phase of a 3-µm fs laser pulse as retrieved from a SHG-FROG trace; also included is the actual MIR spectrum. **c** Measured (*left*) and retrieved (*right*) SHG-FROG traces for the pulse in **b**

adjusted as a zero-dispersion compressor, such that its pulse length remains constant after propagation through this shaper. Now, the spectrum is almost fully blocked in the Fourier plane: only a small central spectral range is transmitted, which determines the idler's final pulse length. Signal and idler beams are temporally and spatially recombined by means of a delay stage and a dichroic mirror, and focussed onto the 1-mm $AgGaS_2$ crystal. The position of the mixing crystal behind the focussing lens is varied to maximize the MIR output and minimize saturation effects. The mixing scheme supports any wavelength from 3 to 10 µm. However, MIR pulse characterization is restricted by sensitivity of detector arrays, crystal absorption or unfavorable phase-matching conditions. Restricting ourselves to the wavelength regime of 3–5 µm, we characterize the pulses with standard autocorrelation (AC) and frequency-resolved optical gating (FROG) techniques. AC is based on frequency doubling in a 100-µm KTP crystal. For the FROG we perform second-harmonic generation (SHG) of the MIR pulses in a 100-µm $AgGaS_2$ crystal and record the spectra with a 256-pixel InGaAs array.

Figure 2a shows exemplary AC measurements for the idler pulse before and after spectral narrowing. The idler AC half-width is broadened to ≈ 2 ps. Although it is routinely used in the NIR and VIS, the application of FROG in the MIR has, to the best of our knowledge, only once been documented in the literature by another group [22]. Therefore, we include a SHG-FROG measurement for a MIR pulse at 3 µm: in Fig. 2c a measured FROG trace and its retrieved version [23] are shown (FROG error $< 0.5\%$). In Fig. 2b, the retrieved spectrum and the true MIR spectrum are compared and found to be in excellent agreement, demonstrating that the doubling crystal in the FROG setup provides a sufficient bandwidth for accurate pulse characterization.

3 Results

In what follows we always generate MIR pulses at $\approx$ 3-µm central wavelength, i.e. the signal pulse is set to ≈ 1.28 µm. The MIR output is maximized by optimizing the temporal overlap between signal and idler, and by tuning the mixing crystal. We concentrate on the generation of multiple-pulse structures in the MIR. To begin with, we generate signal double-pulse structures and mix them with the narrowband idler. Figure 3 shows the resulting FROG traces. Since the idler has no significant chirp, we produce a one-color double pulse, as is confirmed by the fact that all three peaks lie within an equal wavelength range. Within the temporal width of the idler pulse, the temporal separation between the MIR double pulse can easily be varied. It is equal to the distance between the two signal pulses (not shown).

Next, we investigate the possibility of controlling the relative phase of a double pulse. The time separation between the individual pulses is held constant at ≈ 500 fs. We specify the relative phase of the signal double pulses to be 0, $\frac{\pi}{4}$, $\frac{\pi}{2}$, $\frac{3\pi}{4}$ and π. Note that, in SHG-FROG measurements of double-pulse structures, there is generally an ambiguity in the relative phase for φ, $\varphi + \pi$ [24]. Therefore, only phase shifts up to π were imposed. In Fig. 4a the results from the corresponding FROG measurements are shown. In this case, the relative intensities have arbitrarily

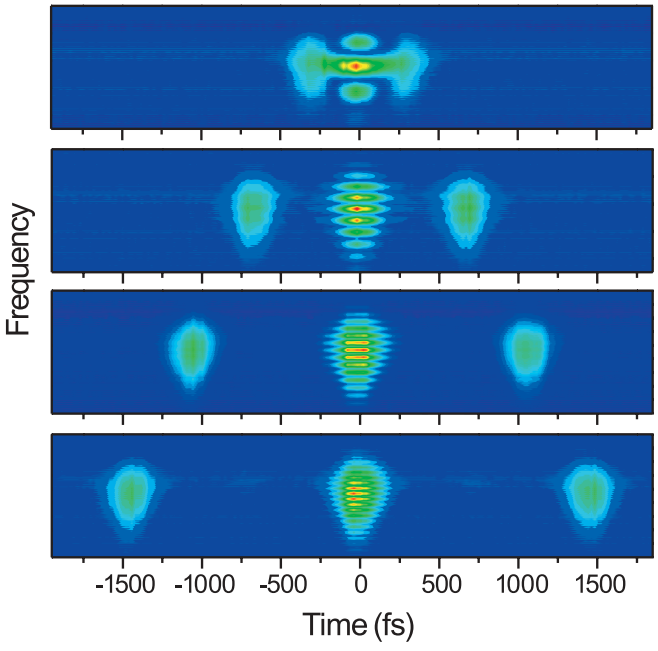

FIGURE 3 Experimental FROG traces for the one-color MIR double pulses at time separations of up to 1.5 ps

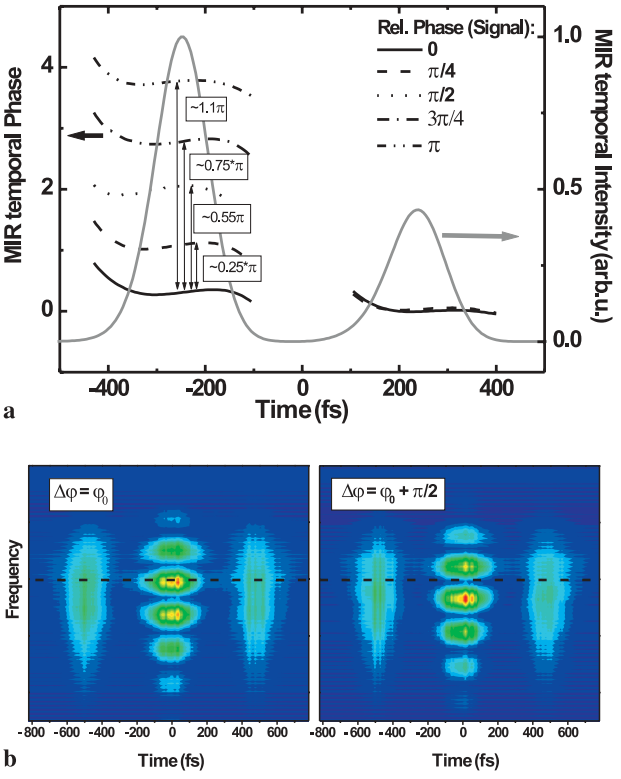

FIGURE 4 **a** Temporal intensity (*right-hand scale*) and phase (*left-hand scale*) for double pulses constant in intensity and time separation, for which the relative phase has been varied by fractions of π. These curves were retrieved from corresponding FROG traces shown (for two cases) in **b** experimental SHG-FROG traces for zero and $\frac{\pi}{2}$ relative phases. Note the shift of the central interference pattern. The imposed relative phase at the signal pulse (*legend*) is identically transferred to the MIR (graphs in **a**)

been chosen to be 1 : 2. This relation is not only dependent on the relative intensity of the signal pulses, but also on the overlap with the envelope of the temporally stretched idler: if this overlap is not symmetric with respect to the idler's intensity maximum, then the generated MIR pulses cannot have identical intensities. Here the important point is the relative phase transfer. Indeed, the relative phase imposed on the signal pulses (legend of Fig. 4a) is truthfully transferred to the MIR double pulse. For zero relative phase of the signal pulses, we find a negligible phase difference between the MIR double pulses, which may indicate a small residual chirp of the idler. In Fig. 4b we show the FROG traces for zero and for $\frac{\pi}{2}$ relative phases. Note that the interference pattern of the central peak, which is typical for any one-color double pulse, is shifted by half a period, as expected. A relative phase of 0 and π would result in identical FROG traces, as mentioned above.

The transfer of pulse sequences with a higher number of subpulses is also possible. In Fig. 5a and b, autocorrelation traces of MIR triple and quadruple pulses are shown together with the AC traces of the controlling signal pulses. Time separation and time profile of signal and MIR pulse sequences closely follow each other. In contrast to the double and triple pulses obtained in [1] with a chirped but not spectrally narrowed idler pulse, the resolution of the shaped MIR transients is much higher with the present scheme. Also shown in Fig. 5c are two FROG traces of a MIR triple pulse, where again the relative phases of the signal pulses have been varied. For the left-hand trace, the relative phases were zero; for the right-hand trace, however, the phase of the central pulse was shifted by $\frac{\pi}{2}$ relative to the other two phases (which both remained zero). As indicated by the dashed line, the interference pattern in the central part of the FROG trace shifts by half a period, as is expected with the phase shift imposed.

An alternative method for the generation of pulse sequences is the application of periodic spectral phase functions [25]. If, for example, the spectral phase in the Fourier plane of the shaper is specified as $\varphi(\omega) = a \sin[b\omega]$, the interspacing of the pulse sequence is determined by the parameter b, and its modulation depth is specified by a. Figure 6a shows the AC traces of a signal and its transfer to 3 μm. The interspacing has been set to be 400 fs. As can be seen, such a structure is conserved during the DFM process. In Fig. 6b a more complex trace, also generated by a sine phase pattern in the NIR, is shown. This AC trace contains 11 intensity peaks, i.e. is generated by a sequence of six subpulses. We point out that, for pulse-sequence generation, periodic phase patterns might be more appropriate since active amplitude modulation by setting transmission factors of mask pixels to values below 1 is avoided,

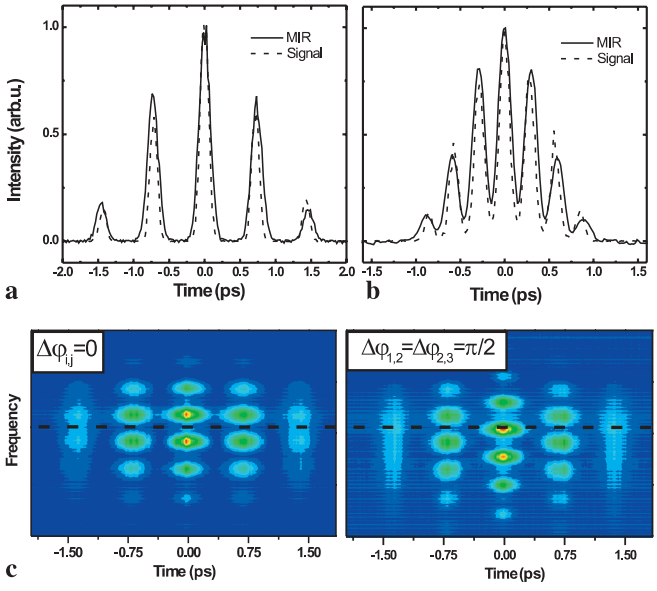

FIGURE 5 **a** AC trace of MIR (*straight line*) and corresponding signal (*dashed line*) pulses. **b** As (**a**), for a quadruple pulse. **c** Experimental FROG traces for a triple pulse with zero relative phases (*left*) and for a triple pulse whose central pulse's phase is relatively shifted by $\frac{\pi}{2}$. The *dashed line* indicates the corresponding shift in the interference pattern

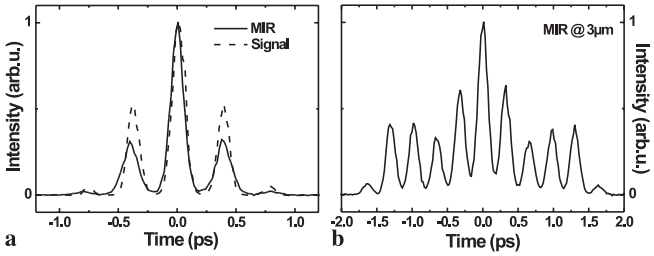

FIGURE 6 Generation of MIR pulse sequences by transfer of sinusoidal spectral phases. In **a** the corresponding signal AC has been included to demonstrate equal subpulse separation. The sequence in **b** consists of six subpulses

leading to higher pulse energies after propagation through the shaper.

4 Summary

Programmable complex MIR pulses can be generated by shifting the shaping process to the near infrared and subsequently transferring modulated pulses to the MIR via difference-frequency mixing. We have demonstrated double and triple pulses with variable delay of up to 1.5 ps and with precisely controllable relative phases. Spectral sine phase functions, which effect multiple-pulse structures, could also be transferred. As two types of more complex pulse shapes, we showed a quadruple pulse as well as a (sine-phase generated) sequence with up to six subpulses. The presented concept is capable of delivering pulses in the 3–10-μm region, which is particularly interesting for molecular vibrational excitation studies. Besides the high resolution of pulse shaping in the 1–1.6-μm wavelength region, the key element to successful MIR pulse shaping is the use of a narrow-band, Fourier-limited idler pulse for the DFM process, which significantly improved the quality and resolution of the resulting MIR transients. This scheme is especially suitable for feedback-controlled coherent control studies, since the pulse characteristics are tuned purely electronically within milliseconds.

ACKNOWLEDGEMENTS

The authors thank D. Proch and D. Zeidler for helpful discussions and K. Bauer for technical assistance.

REFERENCES

1 T. Witte, D. Zeidler, D. Proch, K.L. Kompa, M. Motzkus: Opt. Lett. **27**, 131 (2002)
2 F. Eickemeyer, R.A. Kaindl, M. Woerner, T. Elsaesser, A.M. Weiner: Opt. Lett. **25**, 1472 (2000)
3 H.S. Tan, E. Schreiber, W.S. Warren: Opt. Lett. **27**, 439 (2002)
4 N. Belabas, J.P. Likforman, L. Canioni, B. Bousquet, M. Joffre: Opt. Lett. **26**, 743 (2001)
5 H. Rabitz, R. de Vivie-Riedle, M. Motzkus, K.L. Kompa: Science **288**, 5467 (2001)
6 J.J. Baumberg, A.P. Heberle, K. Koehler, K. Ploog: J. Opt. Soc. Am. B **13**, 1246 (1996)
7 F. Eickemeyer, M. Woerner, A.M. Weiner, T. Elsaesser, R. Hey, K.H. Ploog: Appl. Phys. Lett. **79**, 165 (2001)
8 R.S. Judson, H. Rabitz: Phys. Rev. Lett. **68**, 1500 (1992)
9 T. Witte, T. Hornung, L. Windhorn, D. Proch, R. de Vivie-Riedle, M. Motzkus, K.L. Kompa: J. Chem. Phys. **118**, 2021 (2003)
10 L. Windhorn, J. Yeston, T. Witte, D. Proch, M. Motzkus, W. Fuss, B. Moore, K.L. Kompa: submitted to J. Chem. Phys.
11 M. Hacker, T. Feurer, R. Sauerbrey, T. Lucza, G. Szabo: J. Opt. Soc. Am. B **18**, 866 (2001)
12 E. Zeek, K. Maginnis, S. Backus, M. Murnane, G. Mourou, H. Kapteyn, G. Vdovin: Opt. Lett. **24**, 493 (1999)
13 R.A. Kaindl, M. Wurm, K. Reimann, P. Hamm, A.M. Weiner, M. Wörner: J. Opt. Soc. Am. B **17**, 2086 (2000)
14 G.M.H. Knippels, A.F.G. van der Meer, R.F.X.A.M. Mols, P.W. van Amersfoort, R.B. Vrijen, D.J. Maas, L.D. Noordam: Opt. Commun. **118**, 546 (1995)
15 F. Eickemeyer, R.A. Kaindl, M. Woerner, T. Elsaesser, A.M. Weiner: Opt. Lett. **25**, 1472 (2000)
16 D. Zeidler, T. Witte, D. Proch, M. Motzkus: Opt. Lett. **26**, 1921 (2001)
17 H.S. Tan, W.S. Warren, E. Schreiber: Opt. Lett. **26**, 1812 (2001)
18 G. Veitas, R. Danielius, E. Schreiber: J. Opt. Soc. Am. B **19**, 1411 (2002)
19 The mask was calibrated at 1.29 μm. Our setup features cylindrical mirrors to ensure wavelength-independent imaging, and offset angles are kept at 15° to minimize imaging aberrations
20 A.M. Weiner: Rev. Sci. Instrum. **71**, 1929 (2000)
21 M.M. Wefers, K.A. Nelson: J. Opt. Soc. Am. B **12**, 1343 (1995)
22 B.A. Richman, M.A. Krumbügel, R. Trebino: Opt. Lett. **22**, 721 (1997). Other possibilities for MIR pulse charcterization comprise XFROG (Sibbett and coworkers: Opt. Lett. **25**, 1478 (2000)) and electro-optic sampling (Zhang and coworkers: Appl. Phys. Lett. **71**, 1285 (1997))
23 FROG evaluation software by Femtosoft Technologies, http://www.wco.com/~fsoft
24 R. Trebino, K.W. DeLong, D.N. Fittinghoff, J.N. Sweetser, M.A. Krumbügel, B.A. Richman: Rev. Sci. Instrum. **68**, 3277 (1997)
25 A.M. Weiner, D.E. Leard: Opt. Lett. **15**, 51 (1990)